Theoretical Investigation of the Precipitation of δ' in Al-Li

A. G. KHACHATURYAN, T. F. LINDSEY, and J. W. MORRIS, Jr.

This paper contains the results of a theoretical investigation of the equilibrium between a disordered fcc solution and an $L1_2$ phase in a model binary alloy and the transformation paths that may be followed when the disordered phase is quenched into the two-phase field. The results are specifically applied to binary Al-Li alloys, in which case the ordered phase is the metastable Al_3Li (δ') phase that precipitates from the disordered solid solution (α). The thermodynamic model assumes that the atoms interact in pairs with an interaction potential that is independent of the temperature and composition, and uses the "mean field approximation" for the entropy of mixing. The assumptions confine its applicability to temperatures well below the ordering temperature of the $L1_2$ phase. The model is used to compute the two-phase field that separates the disordered solution and the $L1_2$ phase. For the specific case of Al-Li, it provides results that fit the available experimental data and offer a simple explanation for the observed deviation from stoichiometry of the δ' phase. The model predicts that the disordered solution orders congruently on quenching, but is then unstable with respect to decomposition by a spinodal mechanism that leads ultimately to a state of ordered $L1_2$ precipitates in a disordered matrix. The results provide plausible interpretations for the transformations observed in quenched Al-Li alloys.

I. INTRODUCTION

THE metastable δ' (Al_3Li) phase in the aluminum-lithium system has recently attracted significant interest because of its role as a hardening precipitate in Al-Li alloys. The precipitate has the $L1_2$ structure shown in Figure 1, and forms when a homogeneous α solution is quenched into the metastable two-phase field that is shown in Figure 2.[1] Only the low-temperature portion of the metastable two-phase field has been determined,[2,3] since the solubility of Li in the parent fcc α-phase is limited to approximately 13 at. pct.[4] The stoichiometry of the ordered phase is also uncertain because of the difficulty of extracting the precipitate or analyzing the lithium content *in situ*. The δ' compositions shown on the diagram are taken from low-angle scattering measurements by Cocco *et al.*,[5] and plasmon-EELS studies by Sung, Chan, and Williams,[1] who provide the error bar on the high temperature data point.

The limit of stability of the α solution is also of interest since thermodynamic instabilities may well determine the microstructure of the alloy in the quenched condition. The experimental data (for example, References 3, 5, and 6) suggest that binary alloys with more than about 5.5 at. pct Li always contain small δ' precipitates in the as-quenched state. Dynamic resistivity measurements by Ceresara *et al.*[7] indicate that a homogeneous ordering reaction precedes the formation of discrete δ' particles in a 6.7 pct Li binary.

The only computation of the metastable two-phase field that is known to the authors was done by Sigli and Sanchez,[8] who used a cluster variation technique to achieve an overall fit to the Al-Li phase diagram (shown in Figure 3). While their overall results are reasonable, their calculation of the metastable two-phase field that is of interest here differs from the experimental data in at least three respects. It predicts that the δ' phase that is in equilibrium with the α solid solution is essentially stoichiometric, while the available experimental data show significant deviations from stoichiometry. It predicts that the initial instability on cooling is a spinodal decomposition into two disordered solutions, while the available experimental data show that ordered δ' precipitates are invariably present after quench-

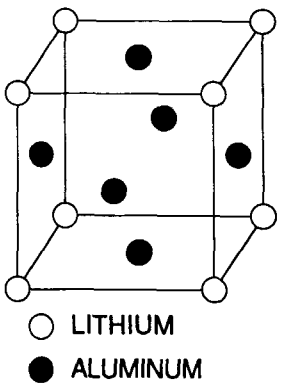

Fig. 1—The $L1_2$ ordered structure of the δ' Al_3Li phase.

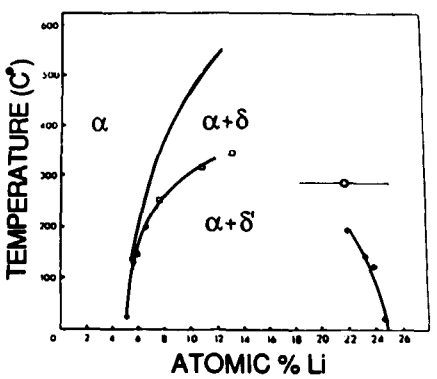

Fig. 2—The metastable two-phase region between the disordered Al-Li solution (α) and the Al_3Li $L1_2$ phase (δ') in Al-Li (after Sung, Chan, and Williams[1]).

A. G. KHACHATURYAN and J. W. MORRIS, Jr. are Professors, Department of Materials Science and Mineral Engineering, University of California, Berkeley, CA 94720. T. F. LINDSEY is Graduate Student Research Assistant, Lawrence Berkeley Laboratory, University of California, Berkeley, CA 94720.

Manuscript submitted December 16, 1986.

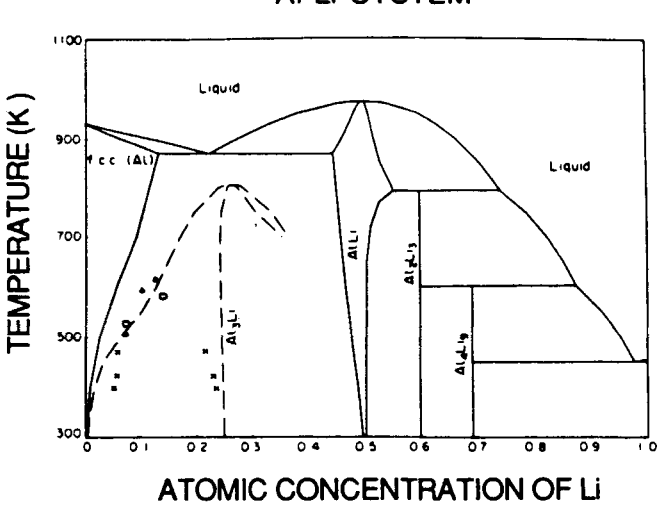

Fig. 3—The aluminum-lithium phase diagram showing the metastable δ' field computed by Sigli and Sanchez.[8]

ing alloys with greater than about 5.5 at. pct lithium. Finally, it predicts an inflection in the metastable α solvus line that is not apparent in the experimental data.

If we confine our attention to the low-temperature portion of the metastable two-phase field, which is the portion of the metastable phase diagram that has greatest practical importance, then it is possible to analyze the metastable two-phase field with a relatively simple and general model. In the limit of low temperature the equilibrium states of both the α solution and the δ' phase must have nearly perfect order. It follows that at sufficiently low temperature the metastable equilibria can be computed in the "mean-field approximation".[9,10,11] Since the mean-field approximation leads to a thermodynamic model that is relatively simple to formulate and use, we employ it to estimate the metastable two-phase field at intermediate temperature. While it is well known that the model leads to erroneous results near the stoichiometric ordering temperature, it should provide a reasonable approximation at lower temperatures where the equilibrium long-range order parameter of the δ' phase is near unity. The mean-field model has the additional advantage that it allows a straightforward analysis of the thermodynamic instabilities the system may encounter.

The particular form of the mean-field model that we shall use places no constraint on the range of the interatomic interaction, but does use the simplifying assumption that the solute atoms interact in pairs. For computational simplicity we make the stronger assumption that the interaction is independent of the composition and temperature.

II. EQUILIBRIUM BETWEEN THE $L1_2$ ORDERED PHASE AND THE DISORDERED SOLID SOLUTION

We wish to find the concentrations, c_α and $c_{\delta'}$, of the disordered solid solution (α) and the $L1_2$ ordered phase (δ') that are in equilibrium at temperature, T, on a fixed fcc lattice. Since the lattice is assumed rigid, the equilibria are governed by the Helmholtz free energy, F. We therefore compute the Helmholtz free energy functions, $F(c,T)$, for the two phases and locate their common tangent. The computation must recognize the fact that the free energy of the ordered phase depends on both its composition and its degree of order (which is specified by the long-range order parameter, η). However, since the long-range order parameter is freely variable, its equilibrium value minimizes the free energy and can be computed as a function of c and T.

A. *The Helmholtz Free Energy*

Let a binary solution be made by distributing atoms of the solvent and solute species over the sites of a face-centered cubic lattice. The configuration of the solution is then specified by the stochastic function, $q(\mathbf{r})$, that takes the value 1 at each lattice site, $\mathbf{r}$, that is occupied by a solute atom and vanishes at all others. If the atoms interact in pairs, the internal energy of the configuration is

$$\begin{aligned} E &= \Sigma_{\mathbf{r}}\, e^\circ q(\mathbf{r}) + (1/2)\Sigma_{\mathbf{r},\mathbf{r}'}\, W(\mathbf{r}-\mathbf{r}')q(\mathbf{r})q(\mathbf{r}') \\ &= N^\circ e^\circ c + (1/2)\Sigma_{\mathbf{r},\mathbf{r}'}\, W(\mathbf{r}-\mathbf{r}')q(\mathbf{r})q(\mathbf{r}') \end{aligned} \quad [1]$$

where the energy is measured relative to that of the pure solvent, N° is the number of lattice sites, e° is the change in energy per atom of solute in the dilute solution limit, c is the atom fraction of the solute, and $W(\mathbf{r}-\mathbf{r}')$ is the effective interaction energy between solute atoms on lattice sites $\mathbf{r}$ and $\mathbf{r}'$.

In the mean field approximation the expected value of the energy of the solution is obtained by averaging Eq. [1] over all configurations that have the average composition, c, while neglecting any correlation between the values of $q(\mathbf{r})$ at $\mathbf{r}$ and $\mathbf{r}'$. The result is

$$E = N^\circ e^\circ c + (1/2)\Sigma_{\mathbf{r},\mathbf{r}'}\, W(\mathbf{r}-\mathbf{r}')c(\mathbf{r})c(\mathbf{r}') \quad [2]$$

where

$$c(\mathbf{r}) = \langle q(\mathbf{r})\rangle \quad [3]$$

is the probability that a solute atom occupies the lattice position at $\mathbf{r}$. The Helmholtz free energy of the solution follows from Eq. [2] and the definition

$$F = E - TS \quad [4]$$

If $W(\mathbf{r}-\mathbf{r}')$ is independent of temperature, the entropy, S, relative to that of the pure solvent is given by the mean field value

$$\begin{aligned} S &= N^\circ s^\circ c \\ &\quad - \mathrm{k}\Sigma_{\mathbf{r}}\,\{c(\mathbf{r})\ln[c(\mathbf{r})] + [1-c(\mathbf{r})]\ln[1-c(\mathbf{r})]\} \end{aligned} \quad [5]$$

where s° is the change in entropy per solute atom in the dilute limit and k is Boltzmann's constant.

For a disordered solution the solute distribution is

$$c(\mathbf{r}) = c \quad [6]$$

and the Helmholtz free energy function is

$$\begin{aligned} F(c,T) &= N^\circ[f^\circ c + (1/2)V(0)c^2] \\ &\quad + N^\circ \mathrm{k}T\{c\ln c + (1-c)\ln(1-c)\} \end{aligned} \quad [7]$$

where $f^\circ = e^\circ - Ts^\circ$ and

$$V(0) = \Sigma_{\mathbf{r}} W(\mathbf{r}) \quad [8]$$

B. *The Free Energy of a Binary System That Includes an $L1_2$ Ordered Phase*

Let a binary system have two possible phases: a disordered solution and an ordered phase with an $L1_2$ structure. A single fundamental equation is sufficient to describe both.

The solute distribution in an ordered phase with the $L1_2$ structure can be written as a superposition of composition waves[12]

$$c(\mathbf{r}) = c + c\eta\{\exp[i\mathbf{k}_1 \cdot \mathbf{r}] + \exp[i\mathbf{k}_2 \cdot \mathbf{r}] + \exp[i\mathbf{k}_3 \cdot \mathbf{r}]\} \quad [9]$$

where η is the long range order parameter and the $\mathbf{k}_i$ are wave vectors in the $\langle 100 \rangle$ directions. Specifically,

$$\mathbf{k}_i = (2\pi/a)\mathbf{e}_i \quad [10]$$

where a is the edge length of the fcc cell and the $\mathbf{e}_i$ are the orthogonal unit vectors [100], [010], and [001]. The directions of the $\mathbf{k}_i$ are the three directions in the star of {100}.

Letting (ξ_1, ξ_2, ξ_3) be the coordinates of the fcc lattice sites,

$$\mathbf{r} = a[\xi_1\mathbf{e}_1 + \xi_2\mathbf{e}_2 + \xi_3\mathbf{e}_3] \quad [11]$$

the solute distribution can also be written in the coordinate form

$$c(\mathbf{r}) = c(\xi_1, \xi_2, \xi_3) = c + c\eta\{\exp[i2\pi\xi_1] + \exp[i2\pi\xi_2] + \exp[i2\pi\xi_3]\} \quad [12]$$

Equation [12] assumes only two values on the fcc lattice sites:

$$c(\mathbf{r}) = c_1 = c(1 + 3\eta) \quad [13]$$

on corner sites of the generic type $(\xi_1, \xi_2, \xi_3) = (0, 0, 1)$, and

$$c(\mathbf{r}) = c_2 = c(1 - \eta) \quad [14]$$

on face-centered sites of the generic type $(0, \frac{1}{2}, \frac{1}{2})$. When the concentration has the stoichiometric value, $c = 1/4$, and the long-range order parameter is 1, $c_1 = 1$ and $c_2 = 0$, which are the appropriate values for the fully ordered $L1_2$ structure shown in Figure 1. When the long-range order parameter is 0, $c(\mathbf{r})$ has the constant value, c, of the disordered solution.

With the help of Eqs. [9], [13], and [14] the Helmholtz free energy of the system can be written as a function of the temperature, concentration, and long-range-order parameter:

$$\begin{aligned} F(T, c, \eta) = {} & (N^\circ/2)\{2f^\circ c + [V(0) + 3V(\mathbf{k}_1)\eta^2]c^2\} \\ & + (N^\circ kT/4)\{c(1 + 3\eta)\ln[c(1 + 3\eta)] \\ & + [1 - c(1 + 3\eta)]\ln[1 - c(1 + 3\eta)] \\ & + 3c(1 - \eta)\ln[c(1 - \eta)] \\ & + 3[1 - c(1 - \eta)]\ln[1 - c(1 - \eta)]\} \end{aligned} \quad [15]$$

where $V(\mathbf{k}_1)$ is the Fourier transform

$$V(\mathbf{k}_1) = \Sigma_r W(\mathbf{r}) \exp(i\mathbf{k}_1 \cdot \mathbf{r}) \quad [16]$$

and we have used the fact that

$$V(\mathbf{k}_1) = V(\mathbf{k}_2) = V(\mathbf{k}_3) \quad [17]$$

When $\eta = 0$ Eq. [15] reduces to Eq. [7], the free energy of the disordered solution. Hence Eq. [15] is sufficiently general to describe both the ordered $L1_2$ structure and the disordered solution.

The equilibrium between the two phases at given T is determined by the common tangent between their free energy curves, $F(c)$, or, equivalently, by the equality of the relative chemical potential of the solute

$$\mu^* = N^{\circ -1}(\partial F/\partial c)_T \quad [18]$$

in the two phases. The linear term in Eq. [15], $N^\circ f^\circ c$, makes the same contribution to the relative chemical potentials of both phases. It is hence sufficient to study the modified free energy function

$$\begin{aligned} f^c(T, c, \eta) = {} & (N^\circ)^{-1}[F - N^\circ f^\circ c] \\ = {} & (1/2)[V(0) + 3V(\mathbf{k}_1)\eta^2]c^2 \\ & + (kT/4)\{c(1 + 3\eta)\ln[c(1 + 3\eta)] \\ & + [1 - c(1 + 3\eta)]\ln[1 - c(1 + 3\eta)] \\ & + 3c(1 - \eta)\ln[c(1 - \eta)] \\ & + 3[1 - c(1 - \eta)]\ln[1 - c(1 - \eta)]\} \end{aligned} \quad [19]$$

The only material parameters that appear in Eq. [19] are $V(0)$ and $V(\mathbf{k}_1)$, which are sufficient to determine the behavior of the system whatever the range of the interatomic interaction.

It is useful to recast Eq. [19] in a dimensionless form. Defining the dimensionless temperature,

$$\tau = kT/|V(\mathbf{k}_1)| \quad [20]$$

and the dimensionless interaction parameter,

$$V^* = V(0)/|V(\mathbf{k}_1)| \quad [21]$$

we have

$$\begin{aligned} f(\tau, c, \eta) = {} & f^c(T, c, \eta)/|V(\mathbf{k}_1)| \\ = {} & [V^* - 3\eta^2](c^2/2) \\ & + (\tau/4)\{c(1 + 3\eta)\ln[c(1 + 3\eta)] \\ & + [1 - c(1 + 3\eta)]\ln[1 - c(1 + 3\eta)] \\ & + 3c(1 - \eta)\ln[c(1 - \eta)] \\ & + 3[1 - c(1 - \eta)]\ln[1 - c(1 - \eta)]\} \end{aligned} \quad [22]$$

where we have assumed $V(\mathbf{k}_1) < 0$.

C. *The Order Parameter*

While the temperature and concentration of the system are external parameters that can be fixed experimentally, the order parameter is affected by spontaneous redistributions of atoms in the interior. It hence evolves to whatever value minimizes the free energy. From Eq. [22] the extrema of the free energy fall at values of η that satisfy the equation

$$4c\eta/\tau = \ln\{(1 + 3\eta) \cdot [1 - c(1 - \eta)]/(1 - \eta)[1 - c(1 + 3\eta)]\} \quad [23]$$

Equation [23] has no simple analytic solution, but can be solved numerically. The solution for a given concentration has the form shown in Figure 4.

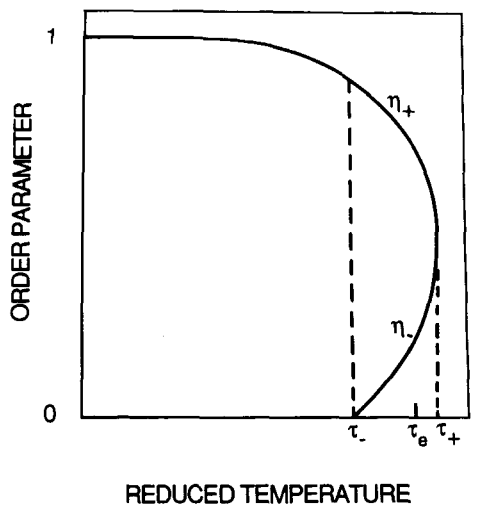

Fig. 4—Schematic variation of the order parameter (η) of the $L1_2$ phase with reduced temperature (τ). The branches η_+ and η_-, and the reference temperatures τ_+, τ_e, and τ_- are defined and discussed in the text.

The behavior of the order parameter is most easily discussed by dividing the temperature axis, τ, into four regimes that are separated by the temperatures τ_+, τ_e, and τ_- indicated in Figure 4. As we shall show below, the temperature τ_- satisfies the equation

$$\tau_- = c(1 - c) \qquad [24]$$

There is no similar analytic form for τ_+ and τ_e. The behavior of η as the temperature decreases is as follows: (1) When $\tau > \tau_+$, $\eta = 0$ and the disordered solution is stable. (2) When $\tau_+ > \tau > \tau_e$ Eq. [23] has three solutions which are, in increasing order, $\eta = 0$, η_-, and η_+. When $\eta = \eta_-$ the free energy is a maximum; the corresponding state is unstable. The solutions at $\eta = 0$ and η_+ are minima. Since the minimum at $\eta = 0$ is the lower of the two, the disordered solution is the preferred phase; the ordered $L1_2$ phase with $\eta = \eta_+$ is metastable. (3) When $\tau_e > \tau > \tau_-$ there are three solutions, $\eta = 0$, η_-, and η_+, but now $\eta = \eta_+$ provides the least value of the free energy. The ordered solution is preferred in this temperature range; the disordered solution is metastable. (4) When $\tau < \tau_-$ there are two solutions, $\eta = 0$ and η_+. The solution at η_+ minimizes the free energy while $\eta = 0$ maximizes it. The ordered solution is stable; the disordered solution is unstable.

It follows that the equilibrium value of the long-range-order parameter is given by the discontinuous function

$$\begin{aligned} \eta(\tau, c) &= \eta_+ \quad [\tau < \tau_e(c)] \\ &= 0 \quad [\tau > \tau_e(c)] \end{aligned} \qquad [25]$$

However, it is also possible to preserve either the ordered phase or the disordered solution in a metastable state beyond the equilibrium ordering temperature. If a disordered solution of composition c is cooled below τ_e it remains metastable until $\tau \leq \tau_-(c)$, at which point it must order spontaneously. If the ordered $L1_2$ phase is heated above τ_e, it remains metastable until $\tau \geq \tau_+(c)$, where it must disorder spontaneously.

D. *The Dimensionless Phase Diagram*

The free energy of the solution is given by the function

$$f(\tau, c) = f[\tau, c, \eta(\tau, c)] \qquad [26]$$

which depends on the material only through the ratio, V^*, of the interaction parameters. For given τ, the function $f_\alpha(\tau, c)$ with $\eta = 0$ generates the free energy curve for the disordered solution (α). It terminates at the composition (c_-) that satisfies the equation

$$\tau = \tau_-(c) = c(1 - c) \qquad [27]$$

since the disordered solution is unstable with respect to long range order when $c \geq c_-$. The function $f_{\delta'}(\tau, c)$ with $\eta = \eta^+$ generates the free energy curve for the $L1_2$ phase (δ'). It terminates at the composition (c_+) that satisfies the equation

$$\tau(c) = \tau_+(c) \qquad [28]$$

where the ordered phase becomes unstable with respect to disorder. The solubility limits are determined by the common tangent,

$$(\partial f_\alpha / \partial c)_T = \mu_e^*(\tau) = (\partial f_{\delta'} / \partial c)_T \qquad [29]$$

$$\frac{f_\alpha - f_{\delta'}}{c_\alpha - c_{\delta'}} = \mu_e^*(\tau) \qquad [30]$$

Example free energy curves for given values of τ and V^* are given in Figure 5 for the composition range of interest, $0 < c < 0.25$. To make the relation between the two curves easy to visualize the function actually plotted in the figure is

$$\omega = f - \mu_e^* c \qquad [31]$$

Figure 5(a) is a schematic plot in which the range of the ordered phase has been exaggerated for clarity. Figure 5(b) is a specific example of the computed results.

Given the free energies of the two phases as functions of τ for given V^*, the two-phase field can be found by locating the common tangent numerically. The results are plotted in Figure 6 for three values of V^*. The plot is terminated at $\tau = 0.18$ since the order parameter of the $L1_2$ phase differs significantly from 1 at higher τ, and the mean field approximation becomes unreliable. The figure shows the breadth of the $L1_2$ phase field, which is greatest at intermediate temperature and increases with the value of V^*.

E. *The α-δ' Two-Phase Field in Al-Li*

To compute the metastable α-δ' two-phase field in the Al-Li binary, we require values for the interaction parameters $V(0)$ and $V(\mathbf{k}_1)$. It is possible to measure the interaction parameters from X-ray diffuse scattering data,[13] but this apparently has not been done for the aluminum-lithium binary. However, it is clear from Figure 6 that the model developed here produces a two-phase field that has the form suggested by the Al-Li data. The best fit is shown in Figure 7, and utilizes the specific values

$$\begin{aligned} V(0)/\mathrm{k} &= 5070\ \mathrm{K} \\ V(\mathbf{k}_1)/\mathrm{k} &= -4060\ \mathrm{K} \end{aligned} \qquad [32]$$

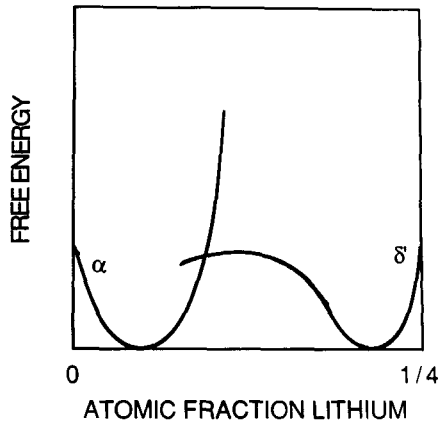

(*a*)

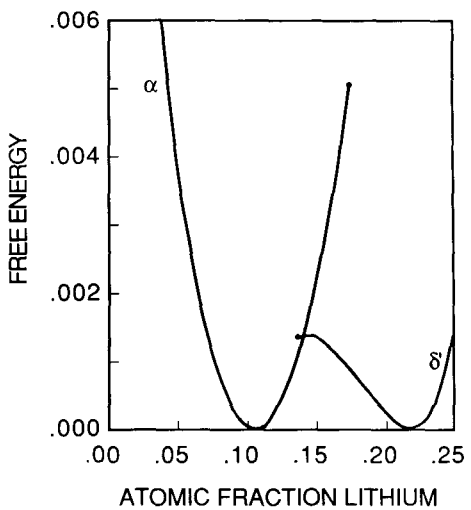

(*b*)

Fig. 5—Free energy curves for the disordered Al-Li solution (α) and the Al_3Li ordered phase (δ'). For clarity, the free energy is measured by the quantity ω (defined in the text) so that the common tangent is along the axis $\omega = 0$. Figure (*a*) is a schematic plot to illustrate the cross-over and instability limits of the two curves. Figure (*b*) is an example of the computed curves.

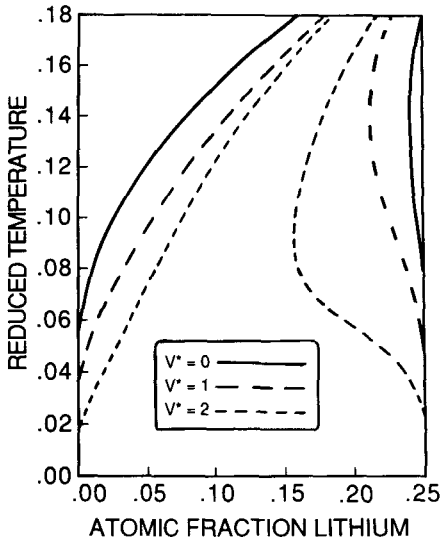

Fig. 6—The boundaries of the two-phase region between a disordered solution and an $L1_2$ ordered phase for three values of the interaction parameter, V^*.

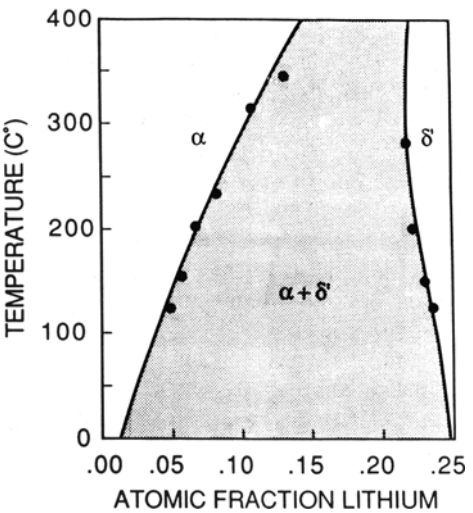

Fig. 7—The computed metastable two-phase ($\alpha + \delta'$) region for Al-Li showing the experimental data. The interaction potentials are $V(0)/k = 5070$ K, $V(\mathbf{k}_1)/k = -4060$ K. For simplicity the error bar on the upper data point on the right-hand side (Fig. 2) has been deleted. (It should be noted that more recent work by Liu and Williams[14] suggests that this data point may lie at lower Li content than is shown here.)

where k is Boltzmann's constant. The two-phase field is not extrapolated to high temperature since the mean-field approximation is unreliable near the ordering temperature.

While the fit to the Al-Li metastable phase field is forced, the results are encouraging in several respects. The predicted phase field matches the experimental data closely on the α side, and simultaneously fits the limited experimental data for the δ' composition. As we shall show below, the model also provides reasonable values for other important properties of the δ' phase. Since the fitted value of $V(0)$ is positive the model automatically predicts that the system orders in preference to decomposition on cooling.

III. NONEQUILIBRIUM REACTIONS

The simple model that is used here has the additional advantage that it allows a straightforward analysis of the various reaction paths a homogeneous solution may take if it is cooled too quickly to permit nucleation of the equilibrium ordered phase. The dominant reactions are those that permit ordering with no change in composition (congruent order). Congruent ordering can happen through the nucleation and growth of ordered domains, or by spontaneous ordering at the limit of stability of the disordered phase (which is the reaction that others have termed "homogeneous order"). The ordered solution may then decompose into the metastable equilibrium phases by the nucleation and growth of Li-rich domains, or by spinodal decomposition on the ordered lattice.

The nonequilibrium reaction paths can be found directly from the shapes of the free energy curves (Figure 5). We can

gain further insight into the nature of the reactions through an analytic treatment of the thermodynamic instabilities the solution may encounter. Since it is fairly simple to identify the reaction paths from the computed free energy curves, we give this discussion first, and then follow it with an analytic description of the order and spinodal instabilities.

The reaction paths are shown schematically in Figure 8 for a hypothetical experiment in which the temperature is fixed and the composition is varied. Let a solution be at temperature T and have the free energy functions shown in Figure 8. Let its composition be increased monotonically from $c = 0$. The disordered solution remains the equilibrium phase until its composition reaches the point D in the diagram, after which it is metastable with respect to nucleation of an ordered phase that has a composition near the composition of the equilibrium ordered phase at point E. The locus of equilibrium compositions for Al-Li is plotted in Figure 7. Now suppose that nucleation is suppressed, for example, by quenching, so that the disordered phase is maintained in a metastable condition. It will eventually reach a set of conditions under which it can order congruently, that is, at constant composition.

A. *Congruent Order*

A disordered solution of composition, c, is metastable with respect to the nucleation and growth of a congruent ordered phase when its composition exceeds the point of intersection of the free energy curves of the α and δ' phases, shown in Figure 8. This intersection occurs when the composition is the solution to the equation

$$\tau = \tau_e(c) \qquad [33]$$

where $\tau_e(c)$ is defined in Figure 4, and corresponds to the congruent transformation temperature, T_0, that is often defined in discussions of phase diagrams. The order parameter of the congruently ordered phase is $\eta_+(c, \tau_e)$. The congruent transformation temperature of the δ' phase in Al-Li is easily computed from the values $V(0)$ and $V(\mathbf{k}_1)$, and is plotted in Figure 9.

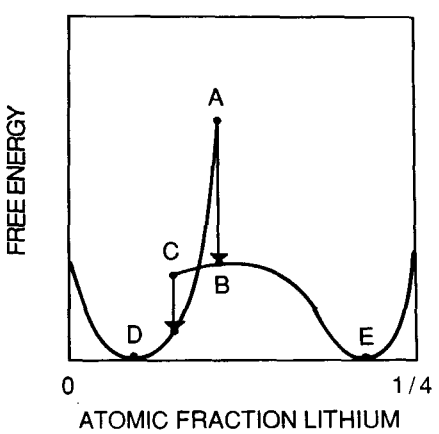

Fig. 8—Schematic drawing showing the cascade of instabilities experienced by a disordered solution of composition A. The solution orders congruently to B, which is unstable with respect to spinodal decomposition. The Li-lean product of the spinodal decomposition evolves to composition C, at which point it is unstable with respect to disorder. The final result includes ordered particles of δ' of composition E in a disordered solution of composition D.

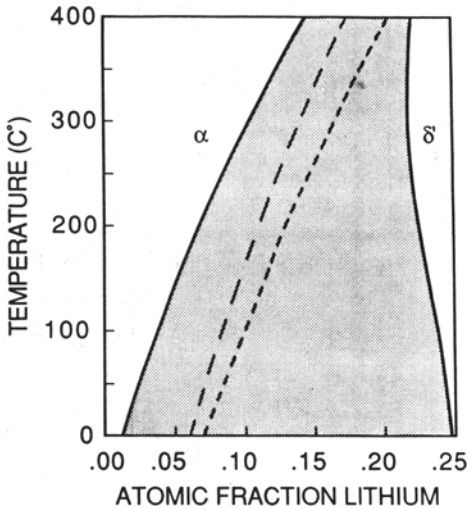

Fig. 9—The metastable two-phase ($\alpha + \delta'$) region in Al-Li showing the computed curves for which a disordered solution is metastable with respect to the congruent nucleation and growth of the ordered phase (between two dash lines) and unstable with respect to spontaneous, homogeneous order (right lower dash line).

If the congruent nucleation of the ordered phase is also prevented, the disordered solution remains stable (its free energy curve is concave) until its composition reaches the point A in Figure 8. It is then unstable with respect to the formation of the composition waves that lead to long-range order ("homogeneous order"). At this point the composition has the value c_-, which corresponds to the point $\tau_-(c)$ in Figure 4. The locus of the ordering instabilities for Al-Li is plotted in Figure 9.

B. *Secondary Decomposition*

If the solution orders congruently, then its composition must evolve further to achieve an equilibrium state. This can happen through the nucleation and growth of one of the equilibrium phases or by the spinodal decomposition of the ordered solution. In the example pictured in Figure 8, which is typical of the results obtained for Al-Li over most of the temperature range studied, congruent order produces a phase whose composition lies in the convex portion of the free energy curve of the ordered phase. The ordered phase is hence unstable with respect to a secondary spinodal decomposition into two ordered phases of different composition. The secondary spinodal is treated analytically in the following section, in which it is shown that the reaction primarily involves the clustering of Al and Li on the Li sublattice of the Al_3Li structure.

In the case of Al-Li spinodal decomposition occurs at all compositions that lie between the inflection point of the δ' free energy curve on the Li-rich side and the termination of the free energy curve on the Al-rich side (Figure 8). The locus of these points is shown in Figure 10.

C. *Secondary Disorder*

In the example shown in Figure 8 congruent order leads to secondary spinodal decomposition that creates adjacent ordered regions that are progressively richer and leaner in Li. But the free energy curve of the ordered phase is convex in the direction of decreasing Li until it terminates at the composition labeled C in the figure. At this point the lean

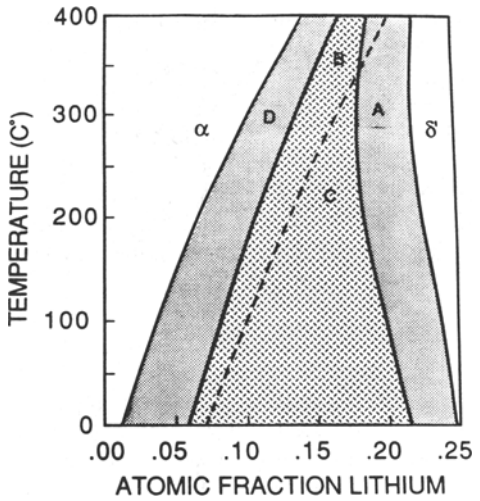

Fig. 10—The metastable two-phase ($\alpha + \delta'$) region in Al-Li showing the computed sub-region (lightly shaded) in which a homogeneously ordered Al_3Li phase is unstable with respect to spinodal decomposition. A solution quenched into the regions marked A and D in the figure is metastable. A solution quenched into the region C orders homogeneously (at the dashed line) and then decomposes through a secondary spinodal. A solution quenched into the region B is metastable with respect to order, but will undergo spinodal decomposition if it orders. Designations of the regions are not related to that of Fig. 8.

phase spontaneously disorders, and its composition evolves further toward the equilibrium state at D.

The composition at the point C corresponds to the point $\tau_+(c)$ that is labeled in Figure 4. The locus of the points of secondary disorder is plotted in Figure 10.

D. *The Nonequilibrium Transformation Path*

It is apparent from Figure 10 that the free energy curves that are drawn in Figure 8 are qualitatively correct for Al-Li for most of the temperature range studied, and are always applicable to the transformation of disordered solutions with less than 13 at. pct Li. If such an alloy is quenched until it orders homogeneously, the sequence of transformations is that indicated by the arrows in Figure 8. The disordered phase spontaneously orders, then decomposes into two ordered phases by a secondary spinodal mechanism. As a consequence of spinodal decomposition, the composition of the Li-lean material eventually reaches the instability point, C, and spontaneously disorders. The expected final microstructure is a mixture of ordered δ' particles in a disordered matrix.

IV. ANALYSIS OF THE INSTABILITY TRANSITIONS

The nonequilibrium transitions that occur in the model system studied here include three that arise from thermodynamic instabilities: homogeneous order, secondary spinodal decomposition, and spontaneous disorder. The first two are amenable to a more detailed analysis that provides further insight into their characteristics.

A. *Homogeneous Order*

Let the composition of the disordered solution be perturbed by an infinitesimal reconfiguration of the solute that is described by the field $\delta c(\mathbf{r})$. The associated change in the Helmholtz free energy is, to second order

$$\delta f^c = (1/2)\Sigma_{\mathbf{r},\mathbf{r}'} A(\mathbf{r},\mathbf{r}')\delta c(\mathbf{r})\delta c(\mathbf{r}') \qquad [34]$$

where

$$A(\mathbf{r},\mathbf{r}') = [\delta^2 f^c\{c(\mathbf{r})\}/\delta c(\mathbf{r})\delta c(\mathbf{r}')] \qquad [35]$$

and the variational derivative is evaluated in the unperturbed state. Substituting Eqs. [2] and [5] into Eq. [4] gives the result

$$A(\mathbf{r},\mathbf{r}') = W(\mathbf{r},\mathbf{r}') + \{kT\delta_{\mathbf{r}\mathbf{r}'}/[c(\mathbf{r})(1 - c(\mathbf{r}))]\} \qquad [36]$$

where $\delta_{\mathbf{r}\mathbf{r}'}$ is the Kronecker delta and $c(\mathbf{r})$ is the unperturbed solute distribution.

According to Eq. [34] a solution is stable with respect to infinitesimal perturbations if the matrix $A(\mathbf{r},\mathbf{r}')$ is positive definite, that is, if all of its eigenvalues, λ, are positive, where the λ are solutions to the equation

$$\Sigma_{\mathbf{r}'} A(\mathbf{r},\mathbf{r}')\delta c(\mathbf{r}') = \lambda\delta c(\mathbf{r}) \qquad [37]$$

The disordered solution, characterized $c(\mathbf{r}) = c$, first loses stability at the temperature at which the least of the λ vanishes. Substituting Eq. [36] into [37] yields an expression for the eigenvalues,

$$\Sigma_{\mathbf{r}'} W(\mathbf{r} - \mathbf{r}')\delta c(\mathbf{r}') + \{kT/[c(1 - c)] - \lambda\}\delta c(\mathbf{r}) = 0 \qquad [38]$$

whose Fourier transform is

$$\{V(\mathbf{k}) + kT/c(1 - c) - \lambda\}\delta c(\mathbf{k}) = 0 \qquad [39]$$

where

$$\delta c(\mathbf{k}) = \Sigma_{\mathbf{r}} \delta c(\mathbf{r}) \exp[-i(\mathbf{k}\mathbf{r})] \qquad [40]$$

It follows that the eigenvalues, λ, are functions of $\mathbf{k}$, T, and c, and satisfy the relation

$$\lambda(\mathbf{k},T,c) = V(\mathbf{k}) + kT/c(1 - c) \qquad [41]$$

The least eigenvalue is associated with the minimum value of $V(\mathbf{k})$, $V(\mathbf{k}^\circ)$, and vanishes at the instability temperature

$$kT_c = -c(1 - c)V(\mathbf{k}^\circ) \qquad [42]$$

If $\mathbf{k}^\circ = \mathbf{0}$ the instability at T_c leads to spinodal decomposition of the disordered solution; if $\mathbf{k}^\circ \neq \mathbf{0}$ the instability leads to spontaneous ordering into the structure determined by the wave vector $\mathbf{k}^\circ$ and the associated wave vectors that are degenerate by symmetry (the vectors of the "star" of $\mathbf{k}^\circ$). In the case of interest here the minima of $V(\mathbf{k})$ fall at the wave vectors $\mathbf{k}_1 = (2\pi/a)\{100\}$ and the disordered solution is first unstable with respect to ordering into the $L1_2$ phase.

B. *Secondary Decomposition of the Ordered Phase*

In the homogeneously ordered phase the eigenvalues of the matrix $A(\mathbf{r},\mathbf{r}')$ are determined by Eq. [38] in the form

$$\Sigma_{\mathbf{r}'} W(\mathbf{r} - \mathbf{r}')\delta c(\mathbf{r}') + \{kT/c(\mathbf{r})(1 - c(\mathbf{r})) - \lambda\}\delta c(\mathbf{r}) = 0 \qquad [43]$$

The solute distribution in the ordered phase, $c(\mathbf{r})$, was given in Eq. [9] in the form of a superposition of concentration waves. The function

$$a(\mathbf{r}) = \{c(\mathbf{r})[1 - c(\mathbf{r})]\}^{-1} \qquad [44]$$

in the second term of Eq. [43] has the same symmetry as $c(\mathbf{r})$ since it is also a measure of composition and must, therefore, be expressible in the same form:

$$a(\mathbf{r}) = \alpha_0 + \alpha_1\{\exp(i\mathbf{k}_1 \cdot \mathbf{r}) + \exp(i\mathbf{k}_2 \cdot \mathbf{r}) + \exp(i\mathbf{k}_3 \cdot \mathbf{r})\} \quad [45]$$

where the $\mathbf{k}_i$ are the wave vectors of type {100} (Eq. [10]). Just as the concentration function, $c(\mathbf{r})$, takes the two values c_1 and c_2 (Eqs. [13] and [14]) on the corners and faces of the unit cell (the Li and Al sublattices, respectively, in δ' Al_3Li), the function $a(\mathbf{r})$ takes the values

$$a_1 = [c_1(1 - c_1)]^{-1} = \alpha_0 + 3\alpha_1 \quad [46]$$

$$a_2 = [c_2(1 - c_2)]^{-1} = \alpha_0 - \alpha_1 \quad [47]$$

on the corners and faces of the parent fcc cell.

Substituting Eq. [45] into [43] and taking the Fourier transform yields the eigenvalue equation

$$[V(\mathbf{k}) + kT\alpha_0 - \lambda]\delta c(\mathbf{k}) + kT\alpha_1[\delta c(\mathbf{k} - \mathbf{k}_1) + \delta c(\mathbf{k} - \mathbf{k}_2) + \delta c(\mathbf{k} - \mathbf{k}_3)] = 0 \quad [48]$$

This equation couples the four variations $\delta c(\mathbf{k})$, $\delta c(\mathbf{k} - \mathbf{k}_1)$, $\delta c(\mathbf{k} - \mathbf{k}_2)$, and $\delta c(\mathbf{k} - \mathbf{k}_3)$. We can obtain three additional equations in these four variables by making the three substitutions $\mathbf{k} \rightarrow \mathbf{k} - \mathbf{k}_i$, $i = 1, 2, 3$ in turn. The result is the matrix equation

$$[A_{\alpha\beta} - \lambda\delta_{\alpha\beta}]\delta c(\mathbf{k}_\beta) = 0 \quad [49]$$

where α and β take the values 1 to 4, $\mathbf{k}_\beta = \mathbf{k} - \mathbf{k}_i$ ($\beta = 1, 2, 3$), $\mathbf{k}_\beta = \mathbf{k}$ ($\beta = 4$), and the matrix elements $A_{\alpha\beta}$ are

$$\begin{aligned} A_{\alpha\beta} &= V(\mathbf{k}_\beta) + kT\alpha_0 \qquad (\alpha = \beta) \\ &= kT\alpha_1 \qquad\qquad (\alpha \neq \beta) \end{aligned} \quad [50]$$

The solutions to Eq. [49] fall at values of λ for which the determinant of the matrix of coefficients vanishes:

$$Det|A_{\alpha\beta} - \lambda\delta_{\alpha\beta}| = 0 \quad [51]$$

Equation [51] is a fourth-order equation in the eigenvalue, λ, and hence has four solutions for each set of wave vectors, $\mathbf{k}_\beta$. Since the matrix is symmetric, all four solutions, λ_σ ($\sigma = 1, \ldots, 4$) are real. Each eigenvalue determines a particular solution that is specified by four values $\delta c(\mathbf{k}_\beta; \sigma)$ ($\beta = 1, \ldots, 4$). It is convenient to define the normalized four-dimensional eigenvector $\mathbf{v}_\sigma(\mathbf{k})$ whose components are $v_\sigma(\mathbf{k}_\beta)$ (that is, $v_\sigma(\mathbf{k} - \mathbf{k}_1)$, $v_\sigma(\mathbf{k} - \mathbf{k}_2)$, $v_\sigma(\mathbf{k} - \mathbf{k}_3)$, $v_\sigma(\mathbf{k})$). The eigenvectors determine the solutions of Eq. [48] according to the relations

$$\delta c(\mathbf{k}_\beta; \sigma) = Q_\sigma(\mathbf{k})v_\sigma(\mathbf{k}_\beta) \quad [52]$$

Then the infinitesimal concentration wave associated with the σth eigenvalue of the matrix $A_{\alpha\beta}(\mathbf{k})$ has amplitude $Q_\sigma(\mathbf{k})$ and is given by

$$\delta c(\mathbf{r}) = Q_\sigma(\mathbf{k})\{\Sigma_\beta[v_\sigma(\mathbf{k}_\beta)\exp(i\mathbf{k}_\beta \cdot \mathbf{r})]\} \quad [53]$$

There is one equation of the form [49] for each independent choice of $\mathbf{k}$, and each equation leads to four eigenvalues, $\lambda_\sigma(\mathbf{k})$. Let the eigenvalues be ordered so that $\lambda_1(\mathbf{k})$ is the least eigenvalue associated with the wave vector $\mathbf{k}$, and let the least of the eigenvalues, $\lambda_1(\mathbf{k})$, be associated with the wave vector $\mathbf{k}^1$:

$$\lambda_1(\mathbf{k}^1) = \text{Min}[\lambda_1(\mathbf{k})] \quad [54]$$

The ordered solution is unstable with respect to an infinitesimal fluctuation in its concentration if $\lambda_1(\mathbf{k}^1) < 0$. The values of the eigenvalues depend on the concentration and the temperature. The division between the stable and unstable fields of the ordered phase in the (c, T) plane is the locus of solutions to the equation

$$\lambda_1(\mathbf{k}^1, T, c) = 0 \quad [55]$$

The type of the instability is determined by the vector $\mathbf{k}^1$. If $\mathbf{k}^1 = 0$ the instability is a spinodal decomposition of the nonstoichiometric ordered phase. If $\mathbf{k}^1 \neq 0$ then the initial instability creates concentration waves that cause a secondary ordering of the nonstoichiometric lattice.

Since we know of no evidence for secondary ordering in Al_3Li, we consider only spinodal decomposition. In this case $\mathbf{k}^1 = 0$ and the matrix $A_{\alpha\beta}$ takes the form

$$\begin{aligned} A_{11} &= A_{22} = A_{33} = V(\mathbf{k}_1) + kT\alpha_0 \\ A_{44} &= V(0) + kT\alpha_0 \\ A_{\alpha\beta} &= kT\alpha_1 \qquad (\alpha \neq \beta) \end{aligned} \quad [56]$$

where we have used Eq. [50] and the identity $V(\mathbf{k}_1) = V(\mathbf{k}_2) = V(\mathbf{k}_3)$. Using Eqs. [56] in [51] the four eigenvalues, $\lambda_\sigma(\mathbf{0})$, can be found, after some algebra, and are:

$$\lambda_1 = [V(\mathbf{0}) + V(\mathbf{k}_1)]/2 - kT(\alpha_0 + \alpha_1) - (1/2)\{[V(\mathbf{k}_1) - V(\mathbf{0}) + 2kT\alpha_1]^2 + 12(kT\alpha_1)^2\}^{1/2} \quad [57]$$

$$\lambda_2 = [V(\mathbf{0}) + V(\mathbf{k}_1)]/2 - kT(\alpha_0 + \alpha_1) + (1/2)\{[V(\mathbf{k}_1) - V(\mathbf{0}) + 2kT\alpha_1]^2 + 12(kT\alpha_1)^2\}^{1/2} \quad [58]$$

$$\lambda_3 = \lambda_4 = -V(\mathbf{k}_1) + kT\alpha_0 \quad [59]$$

An analysis of these equations shows that when the order parameter, η, is non-zero λ_1 is the smallest. The spinodal instability is hence associated with the vanishing of this eigenvalue. When $\lambda_1 = 0$ Eq. [57] can be written as a quadratic equation for T_s, the spinodal instability temperature for given values of c and η. Its positive solution is

$$kT_s = -B/2 + (1/2)[B^2 - 4C]^{1/2} \quad [60]$$

where

$$B = \frac{1}{4}[3V(\mathbf{0}) + V(\mathbf{k}_1)]c_2(1 - c_2) + \frac{1}{4}[V(0) + 3V(\mathbf{k}_1)]c_1(1 - c_1) \quad [61]$$

$$C = V(0)V(\mathbf{k}_1)c_1(1 - c_1)c_2(1 - c_2) \quad [62]$$

The spinodal decomposition limits for the ordered δ' phase in Al-Li are plotted in Figure 10. For the range of temperatures shown, a congruent ordered phase that forms either by nucleation and growth or spontaneous ordering is immediately unstable with respect to spinodal decomposition. It should be impossible to preserve the homogeneously ordered phase; it is immediately decomposes.

To explore the nature of the decomposition we determine the eigenvector associated with the minimal eigenvalue, λ_1. The four-dimensional eigenvector is, in component form,

$$\mathbf{v}_1(\mathbf{k}_1, \mathbf{k}_2, \mathbf{k}_3, \mathbf{0}) = [1 + 3\gamma^2]^{-1/2}(\gamma, \gamma, \gamma, 1) \quad [63]$$

where

$$\gamma = -(\alpha_0/3\alpha_1) - [(V(0) - \lambda_1)/3kT\alpha_1] \quad [64]$$

If this eigenvector is substituted into Eq. [53] for the concentration variation $\delta c(\mathbf{r})$ and the result evaluated on the sites of the fcc parent cell the result is:

$$\begin{aligned} \delta c &= Q_1(0)[1 + 3\gamma^2]^{-1/2}[1 + 3\gamma] \quad \text{(cube corners)} \\ &= Q_1(0)[1 + 3\gamma^2]^{-1/2}[1 - \gamma] \quad \text{(cube faces)} \end{aligned} \quad [65]$$

where the coefficient, γ, is near unity for the range of temperatures of interest here. It follows that the secondary decomposition is principally on the Li sublattice of the δ' structure. The coefficient γ approaches the value 1 as the order parameter, η, approaches 1. When the δ' phase is fully ordered ($\delta c = 0$) on the Al sublattice, and the secondary spinodal is completely confined to the Li sublattice.

The spinodal instability in the limit of low temperature can be understood in terms of the following physical picture. An Al_3Li crystal that is substoichiometric in Li, but fully ordered ($\eta = 1$) has Al atoms on all sites of the Al sublattice, and a mixture of Al and Li atoms on the sites of the Li sublattice. The latter lie at the corners of the fcc unit cell, and hence form a simple cubic lattice. The stability of substoichiometric Al_3Li at $\eta = 1$ is the stability of substitutional solution of Al and Li on a simple cubic lattice with an Li concentration equal to $4c$. It is well known that such a solution has a miscibility gap and undergoes spinodal decomposition on cooling. It follows that substoichiometric Al_3Li undergoes a secondary spinodal decomposition that is confined to the Li sublattice in the limit $\eta = 1$.

V. DISCUSSION AND CONCLUSION

Two sets of results are obtained in this work: those that pertain to the behavior of a model system that contains an $L1_2$ phase and those that specifically concern the metastable $\alpha + \delta'$ field in Al-Li.

A. *The Model System*

Regarding the model system, the results include the general shape of the low-temperature portion of the two-phase field that separates the $L1_2$ phase from the disordered solution and the transformation paths that may be followed when the disordered solution is quenched into the two-phase field.

Perhaps the most interesting result is the cascade of instabilities that is experienced during a quench. The cascade of instabilities is diagrammed in the isothermal free energy plot shown in Figure 8. The temperature of the diagram is that at which the disordered solution first becomes unstable with respect to spontaneous order into the $L1_2$ structure. Hence the system begins from point A in the diagram. Because of the ordering instability its state drops to point B on the $L1_2$ free energy curve. But point B is itself unstable with respect to spinodal decomposition. The spinodal decomposition causes adjacent regions of the solution to change their compositions in opposite directions, as shown by the arrows. The solute-poor phase evolves to point C, at which it is unstable with respect to disorder, and transforms to point D, which lies on the free energy curve for the disordered solution. At the same time the state of the solute-rich phase evolves toward point E, where the ordered phase is stable. If the parent solution has a solute composition well below that of the $L1_2$ phase, which is true in most cases of experimental interest, the final result is a microstructure that consists of islands of ordered phase in a disordered matrix.

Somewhat similar instability cascades have been suggested by a number of authors, principally from analyses of second-order transitions. Allen and Cahn[15] identified a secondary spinodal (which they call a "conditional spinodal") near the second-order transition line in Fe-Al, using a Landau-type free energy expansion that is valid for low values of the long-range order parameter. A detailed analysis of the secondary spinodal associated with a second-order order transition was provided by Kubo and Wayman[16,17] as part of their analysis of the Cu-Al system. They also observed the structures they predicted to arise from the secondary spinodal through high resolution studies of decomposed alloys. Woychik *et al.*[18] have recently provided specific experimental evidence for a homogeneous ordering followed by spinodal decomposition in Cu-Ti solutions. Soffa and Laughlin[19] have recently reviewed relevant data and analyses.

There is also experimental evidence for instability cascades in Ni-based systems that form $L1_2$ phases of the sort treated here. The evidence, which is reviewed by Soffa and Laughlin,[19] is taken primarily from studies of the precipitation of Ni_3Ti in the Ni-Ti system. It should be noted, however, that the schematic free energy curves that Soffa and Laughlin offer to interpret the phenomenon assume continuity between the ordered and disordered states (*i.e.*, that they are related by a second-order transition), and hence do not include the "secondary disorder" phenomenon predicted by the present model (Figure 8).

B. *The Al-Li System*

To evaluate the results that pertain to the Al-Li system, it should be noted that the thermodynamic model that is used here is based on several strong assumptions. The atoms are assumed to interact in pairs through an interaction potential that is independent of temperature and composition and the entropy of the system is evaluated in the mean field approximation. These assumptions necessarily restrict the results to low temperature where the order parameter of the δ' phase is close to unity, and have the consequence that the numerical results are approximate. Nonetheless, the model does provide a good fit to the metastable α-δ' region in Al-Li, and provides a simple explanation for the observation that the δ' phase deviates significantly from its stoichiometric composition. The breadth of the δ' field is a necessary consequence of the fact that the system orders in preference to decomposition at low temperature.

The model also permits a detailed analysis of the transformation paths that may be followed when the α solution is quenched into the metastable $\alpha + \delta'$ field. The model predicts a three-step decomposition sequence. First, the quenched alloy orders congruently, either homogeneously

or through congruent nucleation and growth. Congruent order should always follow sufficiently rapid quenching since the ordering reaction requires only short-range diffusion, and is hence kinetically preferred to the nucleation and growth of the equilibrium phase. Second, the uniformly ordered solution decomposes by a spinodal mechanism into ordered regions that differ in Li content. Third, the low-Li constituent disorders on reaching the limit of stability for the ordered phase. The final microstructure is a mixture of ordered δ' precipitates in a disordered matrix.

The model seems to provide a reasonable picture of the behavior of Al-Li on quenching that is in general agreement with the limited available experimental data. All experimental studies known to the authors conclude that small precipitates form when alloys with greater than about 5.5 at. pct Li are quenched to room temperature. All structural analyses known to the authors conclude that these precipitates are ordered δ' phase. If the quench is done rapidly enough to suppress the nucleation of the metastable equilibrium δ' phase, then the precipitation path must be indirect, as suggested by the results of this investigation.

The studies of Ceresara *et al.*[7] may provide more specific evidence for the picture presented here. They studied the resistivity of as-quenched samples of Al-6.7Li, and observed that the resistivity decreased before increasing to a maximum. Their observations suggest that a long-range ordering reaction precedes the spontaneous formation of discrete precipitates at room temperature. Their results are predicted if the initial reaction is a congruent ordering that is immediately followed by spinodal decomposition of the ordered phase.

The only work of which we are aware that suggests an alternate decomposition scheme is that by Papazian *et al.*,[20] who concluded that the small precipitates present after quenching are Li-rich GP zones that form through spinodal decomposition of the disordered solution. However, this conclusion was based on the coarsening kinetics of the precipitates rather than on their structure. All published work known to the present authors concludes that the system is ordered in the as-quenched condition.

C. *Extensions*

The model can be extended to treat other interesting properties of the δ' phase in Al-Li. For example, the constants $V(0)$ and $V(\mathbf{k}_1)$ that determine the metastable $\alpha + \delta'$ field in the Al-Li phase diagram also determine the first- and second-nearest-neighbor interaction potentials in a model of the alloy in which the range of interaction is confined to second-nearest neighbors. In work that will be published separately we have used the values given in Eq. [32] to estimate the energy of a (111) antiphase boundary in Al_3Li and the energy of the α-δ' interface with results that are in good agreement with experiment.

Finally, the model should also be applicable to other systems that contain ordered phases with the $L1_2$ structure, such as the γ' phase in Fe- and Ni-based superalloys. Some indications of this are contained in the experimental data summarized by Soffa and Laughlin.[19] Its extension to these systems is under investigation.

ACKNOWLEDGMENTS

The authors appreciate helpful discussions with J. Glazer and R. R. Sawtell, Center for Advanced Materials, LBL, and R. J. Rioja, Alcoa Technical Center. They are also grateful to W. A. Soffa of University of Pittsburgh and D. E. Laughlin of Carnegie Mellon University for many valuable discussions, and to the referees for bringing relevant prior work to their attention. This work was supported by the Director, Office of Basic Energy Sciences, Materials Science Division of the United States Department of Energy under Contract No. DE-AC03-76SF00098.

REFERENCES

1. C. M. Sung, H. M. Chan, and D. B. Williams: *Proc., Third International Conference on Aluminum-Lithium Alloys*, C. Baker, P. J. Gregson, S. J. Harris, and C. J. Peel, eds., The Institute of Metals, London, 1986, pp. 337-46.
2. B. Noble and G. E. Thompson: *Metal Science*, 1971, vol. 5, pp. 114-20.
3. D. B. Williams and J. W. Edington: *Metal Science*, 1975, vol. 9, pp. 529-32.
4. A. J. McAllister: *Bull. Alloy Phase Diagrams*, 1982, vol. 3, p. 177.
5. G. Cocco, S. Fagherazzi, and L. Schiffini: *J. Appl. Cryst.*, 1977, vol. 10, pp. 325-27.
6. S. F. Bauman and D. B. Williams: *Acta Metall.*, 1985, vol. 33, pp. 1069-78.
7. S. Ceresara, A. Giarda, and A. Sanchez: *Phil. Mag.*, 1977, vol. 35, pp. 97-110.
8. C. Sigli and J. M. Sanchez: *Acta Metall.*, 1986, vol. 34, pp. 1021-28.
9. A. G. Khachaturyan: *Sov. Phys. Solid State*, 1963, vol. 5, pp. 16-22.
10. A. G. Khachaturyan: *Phys. Stat. Solidi (B)*, 1973, vol. 60, pp. 9-37.
11. V. G. Vaks, A. J. Larkin, and C. A. Pikin: *Zh. Eks. Teor. Fiz.*, 1966, vol. 51, p. 361 (in Russian).
12. A. G. Khachaturyan: *Theory of Structural Transformations in Solids*, J. Wiley and Sons, New York, NY, 1983, p. 46.
13. S. V. Semenovskaya: *Sov. Phys. Solid State*, 1966, vol. 8, p. 2273; *Phys. Stat. Solidi (B)*, 1974, vol. 64, p. 291, p. 627.
14. D. R. Liu and D. B. Williams: *Microbeam Analysis*, A. D. Romig and W. F. Chambers, eds., San Francisco Press, San Francisco, CA, 1986, p. 425.
15. S. M. Allen and J. W. Cahn: *Acta Metall.*, 1975, vol. 23, p. 1017; 1976, vol. 24, p. 425.
16. H. Kubo and C. M. Wayman: *Metall. Trans. A*, 1975, vol. 10A, p. 633.
17. H. Kubo and C. M. Wayman: *Acta Metall.*, 1980, vol. 28, p. 395.
18. C. G. Woychik, R. J. Rioja, T. B. Massalski, and D. E. Laughlin: *Metall. Trans. A*, 1985, vol. 16A, pp. 1353-54.
19. W. A. Soffa and D. E. Laughlin: *Solid State Phase Transformations*, H. Aaronson, D. E. Laughlin, and C. M. Wayman, eds., TMS-AIME, 1981, p. 159.
20. J. M. Papazian, C. Sigli, and J. M. Sanchez: *Scripta Metall.*, 1986, vol. 20, p. 201.